2007 IEEE International Conference on
Robotics and Automation
Roma, Italy, 10-14 April 2007

Robust Nonlinear Fusion of Inertial and Visual Data for position, velocity and attitude estimation of UAV

T. Cheviron, T. Hamel, R. Mahony and G. Baldwin

Abstract— **This paper presents a coupled observer that uses accelerometer, gyrometer and vision sensors to provide estimates of pose and linear velocity for an aerial robotic vehicle. The observer is based on a non-linear complimentary filter framework and incorporates adaptive estimates of measurement bias in gyrometers and accelerometers commonly encountered in low-cost inertial measurement systems. Asymptotic stability of the observer estimates is proved as well as bounded energy of the observer error signals. Experimental data is provided for the proposed filter run on data obtained from an experiment involving a remotely controlled helicopter.**

I. INTRODUCTION

With a range of applications in both civilian and military scenarios, the development of automated aerial robots are an increasingly important field of robotics research. Such vehicles have strong commercial potential in remote surveillance applications such as monitoring traffic congestion, regular inspection of infrastructure such as bridges, dam walls and power cables or investigation of hazardous environments, to name but a few of the possibilities. The development of such robotic vehicles pose a number of unique problems in sensing and control. A key challenge is to develop cheap and robust sensor systems that are light enough to be carried by the vehicle and which provide sufficient information for the vehicle stabilisation. A common sensor suite includes an inertial measurement unit (IMU) consisting of accelerometers and rate gyros, along with a camera. Global positioning systems (GPS) do not function effectively indoors and in urban canyon environments, provide absolute position measurement rather than measurement relative to observed environment and generally do not have sufficient bandwidth for stabilisation of a hovering vehicle. Angular velocity and attitude can be estimated effectively from the output of an IMU system [18], [13], [9] given that the UAV is in quasi-stationary (hover) flight. In contrast, translational position and translational velocity cannot be estimated from a low cost lightweight IMU system for more than a few seconds due to unbounded growth of errors [3]. Vision systems provide a secondary sensor system that can be fused with the IMU data to bound error growth and provide a full state estimate. In recent, years there has been a considerable interest in the development of inertial vision systems [22], [12], [17], [8], [2], [5]. Indeed, there was a session dedicated to such systems at ICRA 2004 [4]. A number of the successful implementations of aerial robotic vehicles over the last few years have relied heavily on vision systems as well as inertial sensor systems [6], [1], [20]. Despite the interest in such systems there is still significant progress to made in the development of detailed results in this area. In this paper, we present a coupled filter algorithm that uses accelerometer, gyrometer and vision sensors to provide estimates of pose and velocity of a rigid body. The algorithm is based on the non-linear complimentary filter framework developed directly in the natural Lie-group geometry on $SO(3)$ [13], [9]. This work in turn draws from earlier work [19], [22], [21] that used a quaternion formulation pioneered in the early nineties. Due to the nonlinear framework, the initialisation of such a filter is less restrictive than a classical Kalman filter and its attractive bassin is extended. Moreover, its implementation requires no observer gain update, which is particulary adapted to low cost embedded smart card. In this paper, we use the vision system to provide the low frequency unbiased measurement of pose and position. The attitude observer is constructed first and is based on the filter developed in Mahony *et al.*[13]. This filter provides an asymptotically stable estimate of the attitude of the vehicle as well as adaptively identifying the gyrometer bias. The novel contribution of the present paper is to prove that the error signals associated with this filter are bounded in the $\mathcal{L}_2$ norm. This is important since these errors form bounded energy disturbances to the proposed position and translational velocity filter. The second stage of the observer uses the vision sensor along with accelerometer readings to provide a filter for the position and translational velocity of the vehicle. Once again we show that closed-loop filter response is asymptotically stable and that the error signals have bounded energy. The filter includes an adaptive dynamic state that estimates the accelerometer bias. The filter has been applied to a data obtained on an experimental platform, a radio controlled helicopter Vario Benzin-Acrobatic 23cc as illustrated on Figure 1, equipped with low-cost, lightweight camera and IMU systems. Results indicate that the proposed observer is effective in estimating the actual pose of the vehicle as well as identifying the gyrometer and accelerometer bias.

T. Cheviron is with LRBA, DGA, Vernon and IRCCyN, UMR 6597, Ecole Centrale de Nantes/CNRS, Nantes, France, Thibault.Cheviron@dga.defense.gov.fr

T. Hamel is with I3S-CNRS Nice-Sophia Antipolis, France, thamel@i3s.unice.fr

R. Mahony is with Departement of Engineering, Australian National University, ACT, 0200, Australia, Robert.Mahony@anu.edu.au

G. Baldwin is with Departement of Engineering, Australian National University, ACT, 0200, Australia, grant.baldwin@anu.edu.au

1-4244-0602-1/07/$20.00 ©2007 IEEE.

II. Problem statement

A. Rigid body dynamical model

Let $\mathcal{I} = \{e_1, e_2, e_3\}$ denote the inertial frame attached to the earth such that e_3 denotes the downwards vertical direction and e_1 points to the magnetic north. Let $\mathcal{B} = \{e_1^b, e_2^b, e_3^b\}$ is a body-fixed frame whose center coincides with the center of mass of the mobile. The attitude of the body-fixed frame is represented by a rotation matrix $R : \mathcal{B} \to \mathcal{I}$. The set of all rotation matrices is termed the Special Orthogonal group and denoted by $SO(3)$. Any $R \in SO(3)$ may be expressed as a rotation of θ radians around an axis $a = (a_1, a_2, a_3)^T \in \mathbb{R}^3$, $||a|| = 1$. The pair (θ, a) is referred to as the angle-axis coordinates of R. Define an operator $(\cdot)_\times$ that maps $a \in \mathbb{R}^3$ into an anti-symmetric matrix via

$$a_\times = \begin{bmatrix} 0 & -a_3 & a_2 \\ a_3 & 0 & -a_1 \\ -a_2 & a_1 & 0 \end{bmatrix}. \tag{1}$$

One has $a_\times b = a \times b$ for any vectors $a, b \in \mathbb{R}^3$ where $\times$ denotes the vector product. Let $\mathrm{vex}(\cdot)$ denote the inverse operation of extracting the vector $a \in \mathbb{R}^3$ from any anti-symmetric matrix $A = a_\times$. One has that $R = \exp \theta a_\times$. Let $\mathbb{P}_a$ and $\mathbb{P}_s$ denote respectively the anti-symmetric and symmetric projection operator in matrix space

$$\mathbb{P}_a(H) = \frac{1}{2}(H - H^T), \qquad \mathbb{P}_s(H) = \frac{1}{2}(H + H^T) \tag{2}$$

For any rotation matrix with angle axis coordinates (θ, a) one has

$$R = I + \sin\theta a_\times + (1 + \cos\theta)a_\times^2 \tag{3a}$$

$$\cos\theta = \frac{1}{2}(\mathrm{tr}(R) - 1) \tag{3b}$$

$$a_\times = \frac{1}{\sin(\theta)}\mathbb{P}_a(R) \tag{3c}$$

Let $\xi_\mathcal{I} = (x, y, z)$ denote the position of the center of mass of the aerial vehicle expressed in frame $\mathcal{I}$. Let $v_\mathcal{I} \in \mathcal{I}$ denote the linear velocity and $\Omega = (p, q, r)$ denote the angular velocity of the airframe with respect to $\mathcal{B}$. The kinematic equation of attitude and Newton's equation of motion yield the following dynamic model for the motion of the rigid body [7]

$$\dot{\xi}_\mathcal{I} = v_\mathcal{I}, \tag{4a}$$

$$m\dot{v}_\mathcal{I} = RF + mge_3, \tag{4b}$$

$$\dot{R} = R\Omega_\times, \tag{4c}$$

where F represents the sum of non gravitational external forces acting on the object and m represents its mass. It is more convenient for the sequel to express the dynamic model (4) in the body fixed frame. Setting $\xi_\mathcal{B} = R^T\xi_\mathcal{I}$ and $v_\mathcal{B} = R^T v_\mathcal{I}$ one has

$$\dot{\xi}_\mathcal{B} = -\Omega_\times \xi_\mathcal{B} + v_\mathcal{B} \tag{5a}$$

$$\dot{v}_\mathcal{B} = -\Omega_\times v_\mathcal{B} + \frac{1}{m}F + gR^T e_3 \tag{5b}$$

$$\dot{R} = R\Omega_\times. \tag{5c}$$

B. Sensor model

We assume that the UAV is equipped with a low cost strap down IMU. Such units are characteristically based on micro electronic-mechanical systems (MEMS) chips and consists of 3-axis accelerometers, 3-axis rate gyrometers and 3-axis magnetometers.

Accelerometers measure all external forces applied to the vehicle, excluding gravity [16]. In case of strap-down IMU, readings are expressed in body fixed frame. Recalling Eq. (5) the pure accelerometer signal is modelled as

$$A_\mathcal{B} = -\Omega_\times v_\mathcal{B} + \frac{F}{m} \tag{6}$$

In practice, the accelerometer measurement, $A^y_\mathcal{B}$, is corrupted by constant (or slowly time varying) bias term, a, as well as Gaussian measurement noise μ_a;

$$A^y_\mathcal{B} = A_\mathcal{B} + a + \mu_a. \tag{7}$$

The angular velocity measurement, Ω^y, is a corrupted measurement of the true angular velocity Ω

$$\Omega^y = \Omega + b + \mu_\Omega, \tag{8}$$

where b represents gyrometer bias and μ_Ω denotes a Gaussian noise process.

In prior work for VTOL UAVs in hover or quasi-stationary flight [13], [9] the accelerometer output was used as an estimate of the negative gravitational vector.

This is valid as long as the vehicle is approximately stationary in the air and external applied force is a thrust that cancels the gravitational force on the vehicle. Averaging the accelerometer readings over a sufficiently long period of time ensures that such an estimate is reasonably accurate, however, if the UAV is engaged in significant manoeuvres this time period may be considerable. Measurement of the magnetic vector field offers some hope of improving the acceleration readings and some works have exploited this structure for [14], [15] to obtain filtered attitude estimates based on reconstruction of the underlying vehicle attitude. However, the magnetometer readings on small UAV systems are often unreliable due to the presence of electric motors and drive systems.

As an alternative to inertial measurements, data from a calibrated camera may be used to deduce precisely the camera's pose with regard to a target of which geometric characteristics are known. A camera is an exteroceptive sensor and provides first order kinematic measurements (ie. attitude and position but not velocity and angular velocity) relative to the observed environment. In contrast to the measurements obtained from inertial sensors, camera measurements are not subject to slowly-time varying biases due to changing temperature and vibration characteristics of the system. Camera calibration is a one of process for which there is a well established and documented toolbox of algorithms. By equipping a UAV with a reasonable quality camera on a good quality and reliable mounting point then it is reasonable to use this data as an aid to pose estimation for manoeuvres where the camera field of view contains a

known target. Examples of such situations are in landing manoeuvres.

Let $\mathcal{C} = \{e_1^c, e_2^c, e_3^c\}$ denote the camera frame attached to the body fixed frame. Let $d_{\mathcal{B}}$ denote the known distance between the center of the camera frame and the center of mass of the vehicle expressed in the the body fixed frame. Let $\mathcal{T} = \{e_1^t, e_2^t, e_3^t\}$ denote the target frame. The target frame is chosen such that its center coincides with the center of mass of the target, which is stationary in the inertial frame.

Using the camera to determine a measurement, R^y, of the attitude matrix on obtains

$$R^y = P_{\mathcal{IT}} R_c R_\mu P_{\mathcal{CB}} \tag{9}$$

where $R_c : \mathcal{C} \to \mathcal{T}$ is the ideal unbiased transformation matrix between the target frame and the camera frame measured by the camera, R_μ is a non Gaussian noise process (assumed to be negligible in the following development) and $P_{\mathcal{CB}}$ and $P_{\mathcal{IT}}$ are two constant transformation matrices that relate the frames of camera measure with the frames of model (4). It is assumed that the matrices $P_{\mathcal{CB}}$ and $P_{\mathcal{IT}}$ are determined in an initial calibration process and are known for the development of the filter theory in the sequel.

A pose estimation algorithm from a calibrated camera also provides an estimate of position of the target $\xi_{\mathcal{C}}$ in the camera frame. Expressing this information in the body fixed frame one obtains

$$\xi_{\mathcal{B}}^y = (R_c P_{\mathcal{CB}})^T \xi_{\mathcal{C}} + d_{\mathcal{B}} + \mu_\xi \tag{10}$$

where μ_ξ is a centered non Gaussian noise process that is assumed to be negligible in the development that follows.

III. Observer design

In this section, two nonlinear observers are proposed. The first observer estimates the orientation matrix and bias terms on the angular velocity observations, the second observer estimates the position and the linear velocity as well as bias terms on the accelerometer observations. A convergence resulting observer is achieved by means of adaptive control and backstepping analysis [11].

A. Nonlinear complementary filter on $SO(3)$

In this subsection, we propose a nonlinear complimentary filter on $SO(3) \times \mathbb{R}^3$ for attitude estimation using visual and 3-axis gyroscope information. The goal is to provide a set of dynamics for an estimate $\hat{R} \in SO(3)$ and $\hat{b} \in \mathbb{R}^3$ to drive the error rotation $\tilde{R} = \hat{R}^T R \to I_3$ and the error bias $\tilde{b} = (b - \hat{b}) \to 0$ given measurements Ω^y and R^y (cf. Eqn's 7 and 9).

Theorem 1: Consider the system given by Eqn's 5. Assume that $\Omega(t) \in L_\infty$ is a bounded continuous signal and assume that gyroscope's bias b is constant or slowly varying. Define observer dynamics in $(\hat{R}, \hat{b})$ by

$$\dot{\hat{R}} = \hat{R}(\Omega^y - \hat{b} + \omega)_\times \tag{11a}$$

$$\omega = l_1 \mathrm{vex}(\mathbb{P}_a(\tilde{R})) \tag{11b}$$

$$\dot{\hat{b}} = -l_2 \mathrm{vex}(\mathbb{P}_a(\tilde{R})) \tag{11c}$$

where l_1 and l_2 are positive gains. Let (θ, a) denote the angle-axis coordinates of the attitude error $\tilde{R}$. Consider the following candidate Lyapunov function

$$V = E_\theta + \frac{1}{4l_2}|\tilde{b}|^2,\ E_\theta = \frac{1}{2}||I_3 - \tilde{R}||_{\mathrm{F}}^2 \tag{12}$$

Where $||M||_{\mathrm{F}} = \sqrt{\mathrm{tr}(MM^T)}$ denotes the Frobenius norm in square matrix space and $|a| = \sqrt{a^T a}$ the euclidian norm in $\mathbb{R}^n$. Then for any positive constant $\delta << 1$ and any initial condition $\hat{R}_0$ such that

$$|\theta_0| \leq \pi - \delta \text{ and that } l_2 > \frac{\tilde{b}(0)}{4(2 - \frac{\delta^2}{2} - E(0))},$$

$\tilde{R} \to I$ and $\tilde{b} \to 0$ asymptotically. Moreover, the error $(\hat{R}, \hat{b})$ is locally exponentially stable to the trajectory $(R(t), b)$ insuring that $||I_3 - \tilde{R}||_{\mathrm{F}}$ and $|\tilde{b}|$ are in $\mathcal{L}_2$.

$$\int_0^\infty ||I_3 - \tilde{R}||_{\mathrm{F}}^2 dt < +\infty, \qquad \int_0^\infty |\tilde{b}|^2 dt < +\infty.$$

Proof: Let us consider the candidate Lyapunov function, Eq. 12

$$V = \frac{1}{2}||I_3 - \tilde{R}||_{\mathrm{F}}^2 + \frac{1}{4l_2}|\tilde{b}|^2 \tag{13}$$

Simplifying the Frobenius norm one obtains

$$V = 3 - \mathrm{tr}(\tilde{R}) + \frac{1}{4l_2}\tilde{b}^T\tilde{b} \tag{14}$$

Recalling (11), the time derivative of $\tilde{R}$ is computed to be

$$\dot{\tilde{R}} = \dot{\hat{R}}^T R + \hat{R}^T \dot{R} = -(\Omega^y - \hat{b} + \omega)_\times \tilde{R} + \tilde{R}\Omega_\times \tag{15}$$

Using the fact that the gyroscope's bias, b, is assumed to be constant or slowly varying and ($\dot{\tilde{b}} = -\dot{\hat{b}}$) and substituting for the sensor model (8) one obtains

$$\dot{\tilde{R}} = -\Omega_\times \tilde{R} + \tilde{R}\Omega_\times - (\omega + \tilde{b})_\times \tilde{R} \tag{16a}$$

$$\dot{\tilde{b}} = l_2 \mathrm{vex}(\mathbb{P}_a(\tilde{R})) \tag{16b}$$

Deriving the Lyapunov function (14) and using (16), one gets

$$\dot{V} = -\mathrm{tr}([\tilde{R}, \Omega_\times]) + \mathrm{tr}((\omega + \tilde{b})_\times)\tilde{R}) + \frac{1}{2l_2}\tilde{b}^T\dot{\tilde{b}} \tag{17}$$

Note that the trace of a matrix commutator is zero and hence $\mathrm{tr}([\tilde{R}, \Omega_\times]) = 0$. Note also, at this point in the equation we have $\tilde{b}^T\dot{\tilde{b}} = 2\mathrm{tr}(\tilde{b}_\times^T \dot{\tilde{b}}_\times)$ and the orthogonality of symmetric and anti-symmetric matrices under the trace operator ensures that $\mathrm{tr}((\omega + \tilde{b})_\times \mathbb{P}_s(\tilde{R})) = 0$. Hence, the time derivative of the candidate Lyapunov function (17) becomes

$$\dot{V} = -\mathrm{tr}\left(\omega_\times^T \mathbb{P}_a(\tilde{R})\right) - \mathrm{tr}\left(\tilde{b}_\times^T(\mathbb{P}_a(\tilde{R}) + \frac{1}{l_2}\dot{\tilde{b}}_\times)\right) \tag{18}$$

Substituting for Eqn's 11b and 11c, then Eq. 18 becomes

$$\dot{V} = -l_1 \mathrm{tr}\left(\mathbb{P}_a(\tilde{R})^T \mathbb{P}_a(\tilde{R})\right) = -l_1 ||\mathbb{P}_a(\tilde{R})||_{\mathrm{F}}^2 \leq 0 \tag{19}$$

This implies that $V(t) \leq V(0)$, and therefore, $\tilde{b}$ is bounded ($\mathbb{P}_a(\tilde{R})$ is always bounded). Since the system (Eq. 16) is not autonomous, Barbalt's lemma is used to conclude the

convergence of the system. To use Barbalat's lemma, let us verify the uniform continuity of $\dot{V}$. The derivative of $\dot{V}$ is :

$$\ddot{V} = -k_P \mathbb{P}_a(\tilde{R})^T \left(\mathbb{P}_a \left([\tilde{R}, \Omega_\times] - \mathbb{P}_a((l_1\omega - \tilde{b})_\times \tilde{R}) \right) \right)$$

This shows that $\ddot{V}$ is bounded, since $\Omega(t) \in L_\infty$ is a bounded continuous signal and $\tilde{b}$ was shown above to be bounded. Hence $\dot{V}$ is uniformly continuous. Application of Barbalat's lemma implies the asymptotic convergence of $\mathbb{P}_a(\tilde{R})$ (or ω) to zero and direct substitution shows that $(\tilde{R}, \tilde{b}) = (I_3, 0)$ is an equilibrium point of Eq. 16.

For local exponential convergence of the solution we study the linearisation of the error dynamics (Eq. 16) at $(I, 0)$. Let $\tilde{R} \approx I_3 + x_\times$ and $\tilde{b} \approx -y$ for $x, y \in \mathbb{R}^3$. The linearised dynamics, obtained after tedious but straightforward calculations, are the time-varying linear system

$$\frac{d}{dt} \begin{pmatrix} x \\ y \end{pmatrix} = \begin{pmatrix} -l_1 I_3 - \Omega(t)_\times & I_3 \\ -l_2 I_3 & 0 \end{pmatrix} \begin{pmatrix} x \\ y \end{pmatrix} \tag{20}$$

Let $|\Omega_{\max}|$ denote the magnitude bound on Ω and choose

$$\alpha_2 > 0, \quad \alpha_1 > \frac{\alpha_2(|\Omega_{\max}| + l_2)}{k_P}, \quad \alpha_3 > \frac{\alpha_1 + \alpha_2 l_1}{l_2}.$$

Set P_R, Q_R to be matrices

$$P_R = \begin{pmatrix} \alpha_1 & \alpha_2 \\ \alpha_2 & \alpha_3 \end{pmatrix}, \quad Q_R = \begin{pmatrix} (\alpha_1 - \alpha_2 l_2) & -\frac{\alpha_2 |\Omega|_{\max}}{2} \\ -\frac{\alpha_2 |\Omega|_{\max}}{2} & \alpha_2 \end{pmatrix}.$$

It is straightforward to verify that P_R and Q_R are positive definite matrices given the constraints on $\{\alpha_1, \alpha_2, \alpha_3\}$. Set $\xi = (x, y)$ then it is a simple matter to verify that

$$\frac{d}{dt} \left(\xi^T P_R \xi \right) < -\xi^T Q_R \xi$$

This proves exponential stability of the linearised system. Finally since the error terms are bounded and uniformly continuous, and the linearised system is exponentially stable, it follows that $||I_3 - \tilde{R}||_{\mathrm{F}}$ and $|\tilde{b}|$ are in $\mathcal{L}_2$. ■

B. Position and Velocity filter

In this subsection, we propose a nonlinear observer for position and linear velocity estimation using visual and 3-axis accelerometer information. The goal is to provide a set of dynamics for an estimates $\hat{\xi}_{\mathcal{B}} \in \mathbb{R}^3$, $\hat{v}_{\mathcal{B}} \in \mathbb{R}^3$ position and translational velocity of the vehicle along with adaptive estimates, $\hat{a} \in \mathbb{R}^3$, of the accelerometer bias.

Given measurements $\xi^y_{\mathcal{B}}$ and $A^y_{\mathcal{B}}$ (cf. Eqn's 7 and 10), we define error signals

$$\begin{aligned} \epsilon_1 &= \xi_{\mathcal{B}} - \hat{\xi}_{\mathcal{B}} \\ \epsilon_2 &= v_{\mathcal{B}} - \hat{v}_{\mathcal{B}} \\ \epsilon_3 &= \hat{a} - a \end{aligned}$$

The goal is to derive filter dynamics that drive these errors to zero.

Theorem 2: Consider the system given by Eqn's 5. Assume that $\xi_{\mathcal{B}}$, $v_{\mathcal{B}}$ and the accelerometer bias a are bounded. Let the filter dynamics for $(\hat{R}, \hat{b})$ be given by Eqn's 11 and let the assumptions of Theorem 1 hold. Define observer dynamics in $(\hat{\xi}_{\mathcal{B}}, \hat{v}_{\mathcal{B}}, \hat{a})$

$$\dot{\hat{\xi}}_{\mathcal{B}} = -(\Omega^y - \hat{b})_\times \hat{\xi}_{\mathcal{B}} + v_{\mathcal{B}} + (k_1 I_3 - (\Omega^y - \hat{b})_\times)(\xi^y_{\mathcal{B}} - \hat{\xi}_{\mathcal{B}}) \tag{21a}$$

$$\dot{\hat{v}}_{\mathcal{B}} = A^y_{\mathcal{B}} - \hat{a} + g\hat{R}^T e_3 + k_2(\xi^y_{\mathcal{B}} - \hat{\xi}_{\mathcal{B}}) \tag{21b}$$

$$\dot{\hat{a}} = -k_3(\xi^y_{\mathcal{B}} - \hat{\xi}_{\mathcal{B}}) \tag{21c}$$

where $k_1, k_2, k_3 \in \mathbb{R}^3$ are constant gains such that $k_3 \neq 0$ and $k_1 k_2 \neq k_3$. Then, the estimates $(\hat{\xi}_{\mathcal{B}},\ \hat{v}_{\mathcal{B}},\ \hat{a})$ are globally asymptotically stable to the true values $(\xi_{\mathcal{B}},\ v_{\mathcal{B}},\ a)$. Furthermore, the error signals $|\epsilon_1|$, $|\epsilon_2|$ and $|\epsilon_3|$ are $\mathcal{L}_2$.

Proof: Combining the dynamics of Eq. 5 and Eq. 21, the error dynamics can be written as

$$\dot{\epsilon_1} = -k_1\epsilon_1 + \epsilon_2 + \tilde{b}_\times \xi_{\mathcal{B}} \tag{22a}$$

$$\dot{\epsilon_2} = -k_2\epsilon_1 + \epsilon_3 + g(I_3 - \tilde{R})R^T e_3 \tag{22b}$$

$$\dot{\epsilon_3} = -k_3\epsilon_1 \tag{22c}$$

Theorem 1 demonstrated finite energy asymptotic stability of the error signals $I_3 - \tilde{R}$ and $\tilde{b}$ to zero. Consequently, $\tilde{b}_\times \hat{\xi}_{\mathcal{B}}$ and $g(I_3 - \tilde{R})R^T e_3$ may be considered as perturbations acting on the error dynamics. This leads to a condensed formulation of Eq. 22

$$\dot{\epsilon} = L\epsilon + \Delta \tag{23}$$

where $\epsilon = (\epsilon_1, \epsilon_2, \epsilon_3)^T$,

$$L = \begin{pmatrix} -k_1 I_3 & I_3 & 0 \\ -k_2 I_3 & 0 & I_3 \\ -k_3 I_3 & 0 & 0 \end{pmatrix}, \quad \Delta = \begin{pmatrix} \tilde{b}_\times \xi_{\mathcal{B}} \\ g(I_3 - \tilde{R})R^T e_3 \\ 0 \end{pmatrix},$$

and Δ is asymptotically decreasing to zero with finite energy. The constant gains $k_1, k_2, k_3 \in \mathbb{R}^3$ are chosen to ensure that L is Hurwitz. To simplify the analysis of stability, set P_ϵ, Q_ϵ to be matrices

$$P_\epsilon = \begin{pmatrix} P_{\epsilon_{11}} & P_{\epsilon_{12}} & P_{\epsilon_{13}} \\ P^T_{\epsilon_{12}} & P_{\epsilon_{22}} & P_{\epsilon_{23}} \\ P^T_{\epsilon_{13}} & P^T_{\epsilon_{23}} & P_{\epsilon_{33}} \end{pmatrix}, \quad Q_\epsilon = \begin{pmatrix} Q_{\epsilon_{11}} & 0 & 0 \\ 0 & Q_{\epsilon_{22}} & 0 \\ 0 & 0 & Q_{\epsilon_{33}} \end{pmatrix}.$$

Expanding the standard Lyapunov function $L^T P_\epsilon + P_\epsilon L = -Q_\epsilon$, it yields to

$$K \begin{pmatrix} P_{\epsilon_{11}} \\ P_{\epsilon_{22}} \\ P_{\epsilon_{33}} \end{pmatrix} = \frac{1}{2} \begin{pmatrix} -Q_{\epsilon_{11}} - k_2 Q_{\epsilon_{22}} \\ Q_{\epsilon_{22}} - k_2 Q_{\epsilon_{33}} \\ -k_1 Q_{\epsilon_{22}} - k_3 Q_{\epsilon_{33}} \end{pmatrix} \tag{24}$$

Set $K = \begin{pmatrix} -k_1 I_3 & k_3 I_3 & 0 \\ 0 & k_1 I_3 & -k_3 I_3 \\ I_3 & -k_2 I_3 & 0 \end{pmatrix}$ and note that $\det K = (k_3(k_1 k_2 - k_3))^3$. By assumption $\det K \neq 0$ and K^{-1} exists. It is now straightforward to find $Q_{\epsilon_{11}}, Q_{\epsilon_{22}}, Q_{\epsilon_{33}}$ positive definite matrices with $k_3 \neq 0$ and $k_1 k_2 \neq k_3$ such that P_ϵ is positive definite, verifying $L^T P_\epsilon + P_\epsilon L = -Q_\epsilon$. Consider the following candidate Lyapunov function

$$S = \epsilon^T P_\epsilon \epsilon \tag{25}$$

Note that for any $X, Y \in \mathbb{R}^{p\times q}$ and $0 < \kappa < \infty$ then $X^T Y \leq \frac{1}{\kappa}|X|^2 + \kappa|Y|^2$. Applying this relation with $X = \Delta$ and $Y = P_\epsilon \epsilon$, the time derivative of S can be written

$$\dot{S} \leq -\epsilon^T Q_\epsilon \epsilon + \frac{1}{\kappa}|\Delta|^2 + \kappa \epsilon^T P_\epsilon^2 \epsilon \tag{26}$$

This leads to

$$\dot{S} \leq -\lambda_1 |\epsilon|^2 + \frac{1}{\kappa}|\Delta|^2 \leq -\lambda_2 S + \frac{1}{\kappa}|\Delta|^2 \tag{27}$$

where $\lambda_{\min}(A)$ (resp. $\lambda_{\max}(A)$) is the smallest (resp. largest) eigenvalue of A, κ is chosen such that $0 < \kappa < \frac{\lambda_{\min}(Q_\epsilon)}{\lambda^2_{\max}(P_\epsilon)}$, $\lambda_1 = \lambda_{\min}(Q_\epsilon) - \kappa\lambda^2_{\max}(P_\epsilon) > 0$ and $0 < \lambda_2 < \frac{\lambda_1}{\sqrt{\lambda_{\min}(P_\epsilon)}}$. Since Δ converges asymptotically to zero, one can ensure ([10], Lemma 4.9, p.208) that S converges to zero. Using the fact that Δ is in $\mathcal{L}_2$, one can deduce ([11], Lemma $B.5$, p.405) that S is in $\mathcal{L}_1$. This guarantees that $|\xi_{\mathcal{B}} - \hat{\xi}_{\mathcal{B}}|$, $|v_{\mathcal{B}} - \hat{v}_{\mathcal{B}}|$ and $|a - \hat{a}|$ are in $\mathcal{L}_2$ and completes the proof. ■

IV. Experimental and simulation results

In this section, we present simulations and experimental results to show the efficiency of the proposed filters. The hardware consists of a 3DMG Microstrain IMU and a Philips webcam mounted on a small scaled helicopter Vario Benzin-Acrobatic 23cc as illustrated on Figure 1. The data is acquired at a rate of $50Hz$ for the inertial sensor and $10Hz$ for the visual sensor.

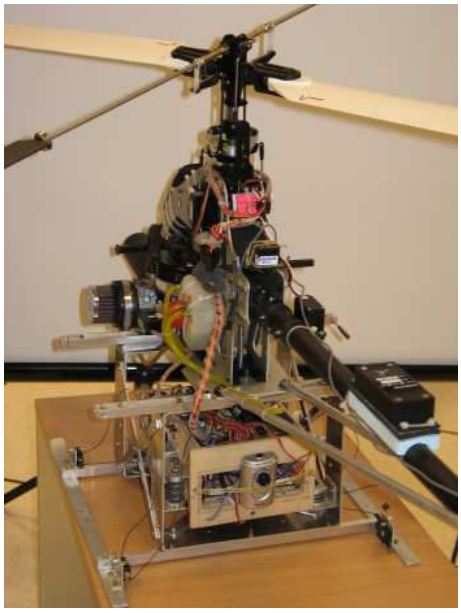

Fig. 1. Experimental platform: a radio controlled helicopter Vario Benzin-Acrobatic 23cc, equipped with low-cost, lightweight camera and IMU systems.

The experiment consists of manual quasi-stationary (or hover) flight over a visual target (ie: a black and white draughtboard). The experiment is conducted such that the target always lies in the field of view of the camera.

The camera calibration has be completed in static condition before the flight. Experimental data obtained during the camera calibration are postprocessed using a recursive least mean square algorithm. The calibration matrices $P_{\mathcal{IT}}$ and $P_{\mathcal{CB}}$ are computed in an initialisation phase. The role/pitch/yaw angles for $P_{\mathcal{IT}}$ are $(1.05°, -1.66°, 164.67°)$ and for $P_{\mathcal{CB}}$ $(-2.4°, -16.83°, 0.1°)$. The gains l_1 and l_2 are tuned to ensure satisfactory asymptotic stability of the linearised dynamics of the nonlinear complimentary filter [14]. The characteristic polynomial of this filter is $\Pi_1(s) = s^2 + l_1 s + l_2$ and observer gains of $l_1 = 15$ and $l_2 = \frac{2}{225}$ are chosen to correspond to a crossover frequency of 0.6Hz and a damping factor of 0.8.

Analogously, we have chosen $k_1 = \alpha + 2\beta$, $k_2 = 2\alpha\beta + \beta^2$ and $k_3 = -\alpha\beta^2$ with $\alpha = 0.01$ and $\beta = 10$ for the nonlinear position and velocity filter such that the characteristic polynomial of the transient matrix L is $\Pi_2(s) = (s+\alpha)(s+\beta)^2$.

The comparison of roll, pitch and yaw angles angles between visual measurements (ie: red cross), inertial measurements using industrial filter of the 3DMG IMU (ie: green curve)and the estimation calculated by the proposed nonlinear complementary attitude filter (ie: blue curve) are shown on Figure 2. Figure 3 illustrates the reconstruction of gyroscopes' bias.

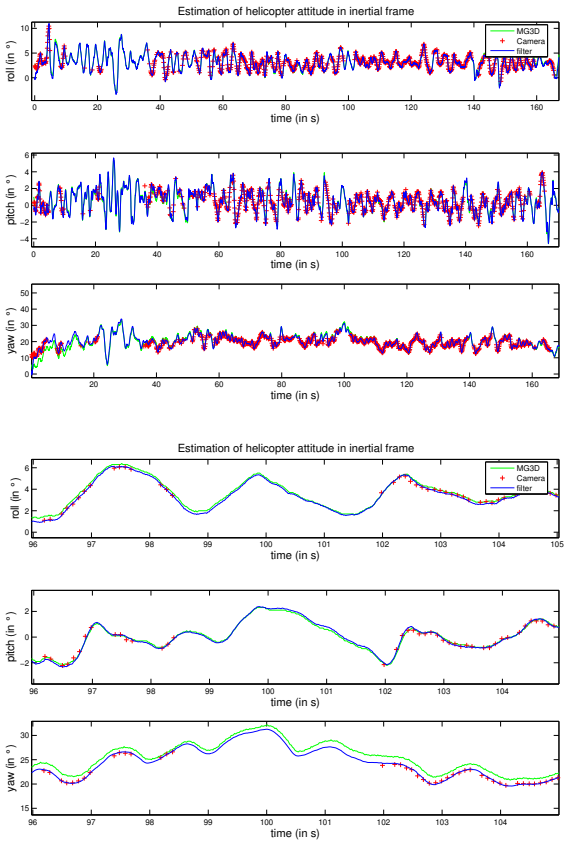

Fig. 2. Estimation of helicopter in inertial frame

The comparison of position between visual measurements (ie: red cross), the estimation calculated by the proposed

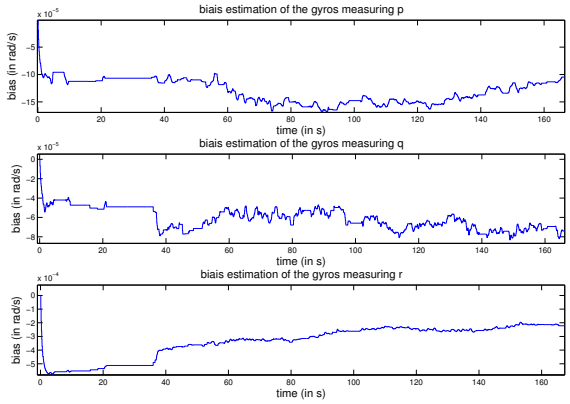

Fig. 3. Estimation of gyroscope bias

nonlinear position filter (ie: blue curve) and the open loop integrated inertial accelerations of the 3DMG IMU (ie: green curve) are shown on Figure 4. Figure 5 and Figure 6 illustrates respectively the reconstruction of linear helicopter velocity and accelerometer' bias.

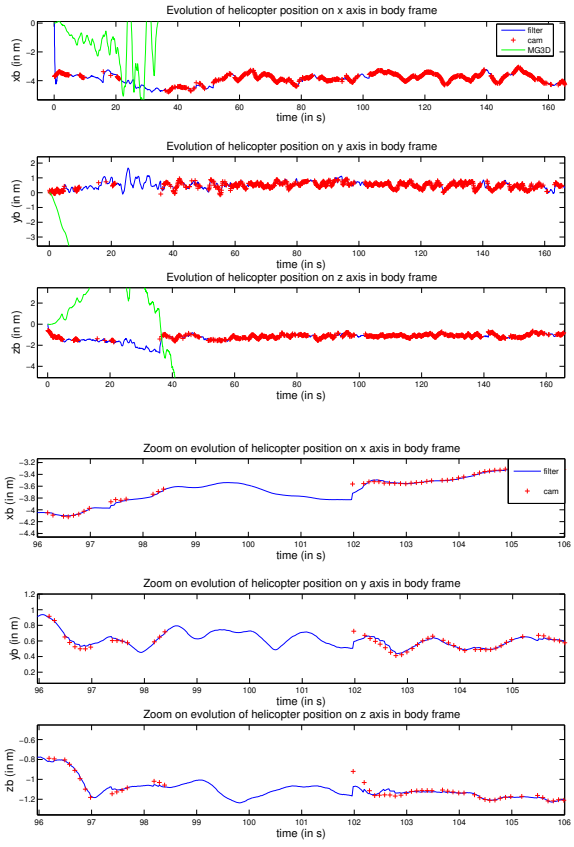

Fig. 4. Estimation of helicopter position expressed in body frame

Excellent behavior of both observers is observed despite the large errors between initial conditions, inertial sensor drift and occasional lack of visual measurements due to non-detection of the target. Figure 2, 4 and 5 prove that accurate exteroceptive visual measurements allows successful estimates of the inertial drift due to gyro and accelerometer bias.

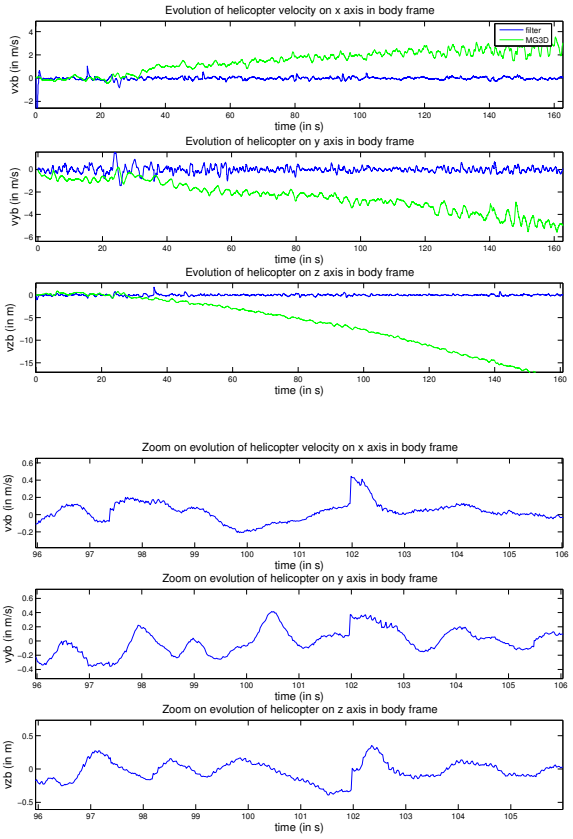

Fig. 5. Estimation of linear helicopter velocity expressed in body frame

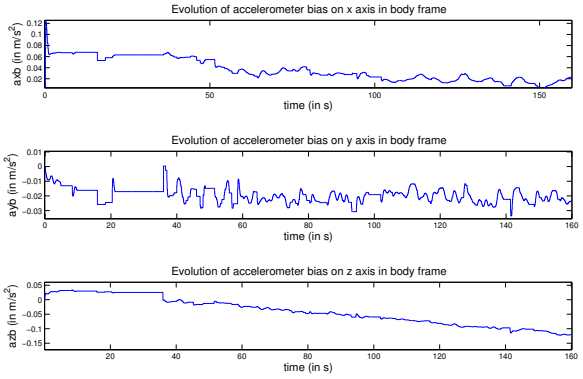

Fig. 6. Estimation of accelerometer bias

V. Acknowledgements

The authors would like to thank Gael Desilles, Johann Forgeard and the whole team of the Autonomous Navigation Laboratory of LRBA for their useful advice. This work is in line with a Ph.D. thesis supported by DGA and in collaboration with IRCCyN.

REFERENCES

[1] O. Amidi, T. Kanade, and R. Miller. *Vision-based autonomous helicopter research at Carnegie Mellon robotics institute (1991-1998)*, chapter 15, pages 221–232. IEEE press and SPIE Optical Engineering press, New York, USA, 1999. Edited by M. Vincze and G. D. Hager.

[2] L. Armesto, S. Chroust, M. Vincze, and J. Tornero. Multi-rate fusion with vision and inertial sensors. In *Proceedings of the IEEE International Conference on Robotics and Automation, ICRA'04*, volume 1, pages 193–199, May 2004.

[3] M. Bryson and S. Sukkarieh. Vehicle model aided inertial navigation for a UAV using low-cost sensors. In *Proceedings of the Australasian Conference on Robotics and Automation*, http://www.araa.asn.au/acra/acra2004/index.html (visited 7 March 2005), 2004. Australian Robotics and Automation Association.

[4] P. Corke, J. Dias, M. Vincze, and J. Lobo. Integration of vision and inertial sensors. In *Proceedings of the IEEE International Conference on Robotics and Automation, ICRA '04.*, number W-M04, Barcellona, Spain, April 2004. Full day Workshop.

[5] Peter Corke. An inertial and visual sensing system for a small autonomous helicopter. *J. Robotic Systems*, 21(2):43–51, February 2004.

[6] E. Frazzoli, M.A. Dahleh, and E. Feron. *Advances in Systems Theory*, chapter A Hybrid Control Architecture for Aggressive Maneuvering of Autonomous Aerial Vehicles. Kluwer Academic Publishers, 1999.

[7] H. Goldstein. *Classical Mechanics*. Addison-Wesley Series in Physics. Addison-Wesley, U.S.A., second edition, 1980.

[8] M. Grimm and R.-R. Grigat. Real-time hybrid pose estimation from vision and inertial data. In *Proceedings of First Canadian Conference on Computer and Robot Vision*, pages 480–486, May 2004.

[9] T. Hamel and R. Mahony. Attitude estimation on $SO(3)$ based on direct inertial measurements. In *International Conference on Robotics and Automation, ICRA2006*, pages –, Orlando Fl., USA, April 2006. Institue of Electrical and Electronic Engineers.

[10] Hassan K. Khalil. *Nonlinear systems*. Macmillan Publishing Company, 1992.

[11] M Krstic, I Kanellakopoulos, and P V Kokotovic. *Nonlinear and Adaptive Control Design*. American Mathematical Society, Providence, Rhode Island, U.S.A., 1995.

[12] J. Lobo and J. Dias. Vision and inertial sensor cooperation using gravity as a vertical reference. *IEEE Transactions on Pattern Analysis and Machine Intelligence*, 25(12):1597–1608, Dec. 2003.

[13] R. Mahony, T. Hamel, and Jean-Michel Pflimlin. Complimentary filter design on the special orthogonal group $SO(3)$. In *Proceedings of the IEEE Conference on Decision and Control, CDC05*, Seville, Spain, December 2005. Institue of Electrical and Electronic Engineers.

[14] N. Metni, J.-M. Pflimlin, T. Hamel, and P. Soueres. Attitude and gyro bias estimation for a flying uav. In *Intelligent Robots and Systems, 2005. (IROS 2005). 2005 IEEE/RSJ International Conference on*, pages 1114–1120, 2-6 Aug. 2005.

[15] J-P. Pflimlin, T.Hamel, P. Soures, and N. Metni. Nonlinear attitude and gyroscope's bias estimation for a VTOL UAV. In *Proceedings of the IFAC World Conference, IFAC2005*, 2005.

[16] J.C. Radix. *Systmes inertiels composants lis strap-down*. Cepadues Edition, 1980.

[17] H. Rehbinder and B.K. Ghosh. Pose estimation using line-based dynamic vision and inertial sensors. *IEEE Transactions on Automatic Control*, 48(2):186–199, Feb. 2003.

[18] J. Roberts, P. Corke, and G. Buskey. Low-cost flight control system for a small autonomous helicopter. In *Proceedings of the Australasian Conference on Robotics and Automation, ACRA02*, Auckland, New-Zealand, 2002.

[19] S. Salcudean. A globally convergent angular velocity observer for rigid body motion. *IEEE Transactions on Automatic Control*, 46, no 12:1493–1497, 1991.

[20] S. Saripalli, J.M. Roberts, P.I. Corke, and G. Buskey. A tale of two helicopters. In *Proceedings of the IEEE/RSJ Intertnational Conference on Intelligent Robots and Systems*, pages 805–810, Las Vegas, Oct. 2003.

[21] J. Thienel and R. M. Sanner. A coupled nonlinear spacecraft attitude controller and observer with an unknow constant gyro bias and gyro noise. *IEEE Transactions on Automatic Control*, 48(11):2011 – 2015, Nov. 2003.

[22] B Vik and T. Fossen. A nonlinear observer for GPS and INS integration. In *Proceedings of the 40th IEEE Conference on Decision and Control*, 2001.